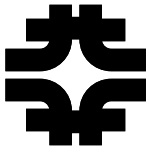

Fermilab

J. MacLachlan, Fermilab, BD/AI 4 December 2003

Evaluation of Longitudinal Emittance Growth Caused by Negative Mass Instability in Proton Synchrotrons

- Negative mass instability (NMI) theory considered satisfactory [W. Hardt 1974]
- Linear perturbation predictions
- Both beam observation and model confirmations difficult and practically non-existent
- Modeling now possible to validate theory and extend calculations to complications of practical cases

Main Points

- Linearized Vlasov analysis makes clear predictions but not one on end-state emittance
- Macroparticle models have been and are even now limited in bandwidth
- Commodity computer clusters now adequate to support credible modeling
- Parallel code for models can be validated independently of agreement with existing theory
- Results of modeling have practical uses

Introduction

- Most proton synchrotrons pass through an energy (E_T) at which the particle circulation frequency is practically independent of momentum differences within beam bunches. At this transition energy $\frac{\partial \omega_{\mathrm{circ}}}{\partial E}$ is zero — positive below E_{T}, negative above.

- Interparticle repulsion causes charge concentrations to disperse below transition but to concentrate above. Near transition, fluctuations in density are practically fixed in the bunch; particles in charge surplus regions push one another to higher and lower energy without much change in relative azimuth.

- If these perturbations constitute a sufficient peak current, the resulting field promotes charge concentration so that bunch grows significantly within a few beam turns, a disruption called negative mass instability (NMI).

- There must be a perturbation of ideal smoothness of charge distribution to start with.

- Usual assumption is that statistical fluctuation arising from discreteness of charge carriers is the seed for instability.

- In practice, stronger perturbations are expected at larger scale.

- Modeling is an excellent way to explore whether such microstructure makes an important contribution to instability.

Heuristic Model for NMI

Gives same threshold criterion as the perturbation calculation and an intuitive idea why amount of noise in seed is not highly critical but initial bunch emittance is. At wavelengths much shorter than bunch length, Fourier spectrum of beam current is white noise. Calculate the energy extent (bucket height) of stable oscillation areas separately for each current component and spacecharge impedance

$$\frac{Z_{\|}}{n} = -i\frac{Z_{\circ} g}{2\beta\gamma^2} \quad : \tag{1}$$

$$V_n = Z_{\|} I_n \tag{2}$$

and consequently a microbucket height in eV

$$H_{\mu\mathrm{B},\,n} = \beta\sqrt{\frac{2eV_nE}{\pi n|\eta|}} \quad , \tag{3}$$

where β and γ are relativistic kinematic parameters, $Z_{\circ}$ is free-space impedance of 376.7 Ω, I_n is n^{th} harmonic peak current, e is magnitude of electron charge, E is proton total energy, n is harmonic number with respect to beam circulation frequency, and η is the phase slip factor $\gamma_T^{-2} - \gamma^{-2}$. Oscillation in mode n will be unstable if microbucket height exceeds bunch height

$$H_{\mu\mathrm{B},\,n} > H_b \quad . \tag{4}$$

However, because $Z_{\|}$ is proportional to n and $H_{\mu\mathrm{B},\,n}$ depends on V_n/n, all modes appear unstable.

Growth rate of instability is given by small amplitude oscillation frequency in the microbuckets

$$\lambda_{\mathsf{rise},\,n} = \sqrt{\frac{n|\eta|eV_n}{2\pi\beta^2 E}} f_\circ \quad . \tag{5}$$

Thus, higher frequency modes grow faster and dominate the disruption.

Because instability appears first at peak current part of bunch, current to be used in calculating I_n is $\widehat{I} = \bar{I}_{\mathsf{bunch}}/B$, where B is the convetional bunching factor. In high frequency range the current can be thought of as a sum of δ-functions of moving charge so each amplitude has a frequency-independent factor of two from Fourier expansion of δ-functions. Plausibly,

$$I_n = 2\bar{I}_{\mathsf{bunch}}/B \quad , \tag{6}$$

and with this choice stability threshold criterion of eq. 4 gives same results as the perturbation calculation.

Noise harmonics weaker than harmonics in expansion of bunch envelope are stable. Heuristic model, however, does not include any limit on effect of very high frequency components, although at least one such limiting factor is effective, namely rolloff of geometrical factor g. At a harmonic $n_{1/2}$ (see Table I) it is one half of its low frequency value.[W. Hardt, 1974]

Nonetheless, one may understand sharpness of emittance threshold in terms of whether microbuckets are higher than bunch or not and insensitivity to bandwidth limitation in terms of simultaneous instability of a wide range of modes. Empirically, final bunch disruption is similar over a wide range of high frequency cutoffs. Even two octaves less than bandwidth indicated in perturbation calculation gives similar end-state results.

Modeling Code and Theory-Independent Validation

The basis of the code used for NMI modeling is a 2-dimensional macroparticle tracking program ESME[J. MacLachlan, 1998] which has evolved and has been extensively used about 20 years. Validating a parallel version for very large distributions is possible without essential need for comparison to the NMI theory or other beam dynamics results, especially because the base code has been validated in many contexts. There is little need for global optimization, because for large number of macroparticles, n_p, computing time is used almost entirely within a single-particle dynamics tracking loop. For $n_p >\sim 10^6$ computing time has scaled almost linearly with n_p and is within a few percent of time scaled from single-processor runs of original ESME. The critical checks are mostly of a numerical sort; for example

1. stability with respect to moderate changes in n_p

2. stability with respect to change in seed for random number generator

3. stability with respect to change from time domain to frequency domain calculation

4. bench marking against another code where both are applicable

Not only did these checks provide a measure of reassurance but indicated in addition that results obtained at 4096 bins/rf period were numerically significant even though the macroparticle statistics were marginal at this finest binning employed. The significance of the highest bandwidth results was inferred from a special result concerning $\frac{\mathrm{d}\lambda}{\mathrm{d}t}$ when evaluated by a three-point formula,[J. Wei, 1992] *viz*., that the numerical noise per bin is the same when the number of bins is doubled if n_p is increased by a factor of 2^3. A sequence of otherwise identical cases was modeled at 512 bins/rf period. In each, n_p was reduced by a factor of eight from the preceding case. From $6.4 \cdot 10^8$, n_p was reduced in steps to $1.28 \cdot 10^6$, where a difference of a few percent appeared in the strength of the most strongly excited Fourier amplitudes and also in the final emittance.

From the fact that the first two reductions in n_p had no significant effect on results, the cubic binning rule implies that 2048 bins are satisfactory with the given n_p, but the step to 4096 needed to cover much of the range of interest according to the perturbation analysis will increase the numerical noise per bin enough to have some effect on results. The differences associated with the final step in the sequence of reductions in n_p are small enough to suggest that results at 4096 bins per rf period are accurate to the few percent level.

However, other checks were made, including runs with different seeds and runs with time domain and frequency domain evaluation of $\frac{\mathrm{d}\lambda}{\mathrm{d}t}$, to confirm this inference. The narrow bandwidth calculation also permitted a direct check on the correctness of the space charge potential calculation. Because the first 256 rf harmonics represent primarily the overall bunch shape but not its finer structure, the voltage calculated by the program for an elliptical distribution was compared to a simple hand calculation. Finally, at n_p accessible to ESME, results were identical to those from the parallel code.

Eq. 5 implies a limitation on macroparticle models which assume that the current distribution remains practically unchanged over a beam turn, a very common ansatz in particle tracking models. The object of study is an instability which causes significant bunch disruption within a small number of beam turns. To extend the calculation to higher frequencies it may become necessary at some point to re-compute the beam current spectrum more than once per turn. However, for the examples used, the rise times are $\mathcal{O}(100)$ beam turns, and the fidelity of the charge distributions should therefore be adequate.

Emittance Threshold in Fermilab Main Injector

The figure following shows the factor by which bunch size grows *vs*. initial bunch size for very high intensity ($2 \cdot 10^{11}$ protons) bunches in the FMI. The vertical dotted line is the analytic stability threshold. This sequence of results tests the analytic result in a particular regime and gives practical guidance to the amount of end-state growth to expect in the vicinity of threshold. The next table displays the parameters used; the per-bunch intensity is usually $\leq 6 \cdot 10^{10}$ protons.

Table I: **Fermilab Main Injector Parameters**

Parameter	Symbol	
Circumference	C	3319.42 m
transition energy/$m_\circ c^2$	γ_T	21.84
rf peak voltage	V_{rf}	3.7 MV
rf harmonic	h	588
beam circulation frequency	$f_\circ$	90.2195 kHz
ramp rate	$\dot{\gamma}$	240.0 s^{-1}
synchronous phase	ϕ_{s}	42.38 deg
nonadiabatic time	T_{na}	1.76 ms
beampipe radius	b	2.5 cm
beam radius	a	0.4 cm
geometric factor	$g_\circ$	4.66
harmonic of $f_\circ$ for $g = \frac{1}{2}g_\circ$	$n_{1/2}$	2238395
number of protons per bunch	N	$2.0 \cdot 10^{11}$
average bunch current	$\bar{I}_{\mathsf{bunch}}$	1.7 A

Emittance Growth Factor *vs*. Initial Emittance for FMI

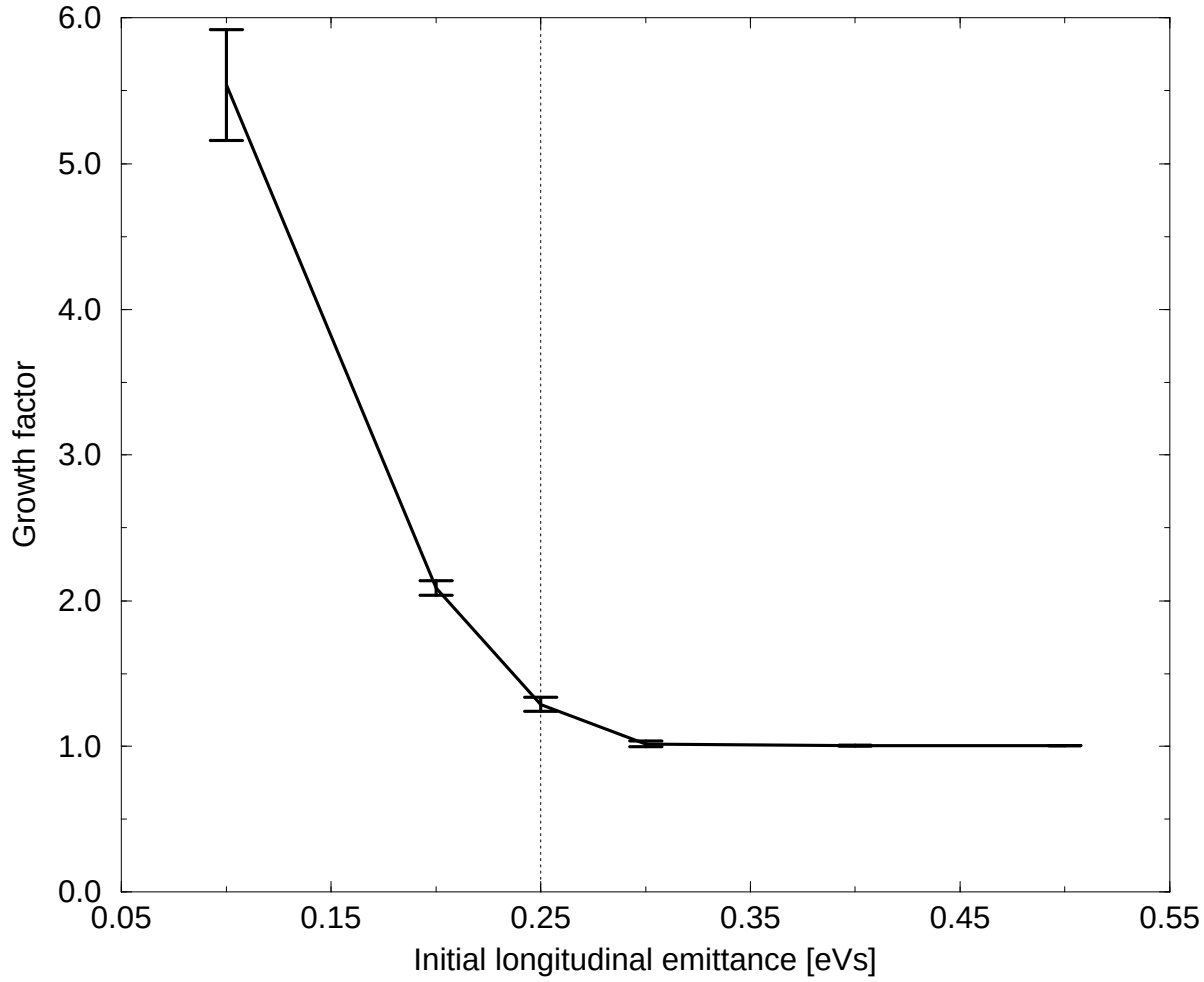

Emittance growth factor *vs*. initial emittance [eVs] for bunches of $2 \cdot 10^{11}$ protons crossing transition in the FMI. Each point is determined by a tracking with $6.4 \cdot 10^{8}$ macroparticles and a run with 10^{8}. The statistically weighted mean is the central value with error bars given by the difference between the two runs. The vertical dashed line is the NMI threshold evaluated either from Hardt's perturbation calculation or the self-bunching criterion.

Fermilab Booster Injector

In distinction to FMI it appears that the Fermilab Booster is marginally unstable with current parameters; this accelerator has become a center of attention within the last year or two as Fermilab works to solve its so-called proton economics problem. The Booster parameters are given in the following Table II. The emittance growth through the acceleration cycle is shown in the following figure. As in practice, it is not simple to unfold the effects of NMI and nonlinear single particle dynamics in the emittance growth near transition. However, there is an estimate of the nonlinear dynamics contribution [Jie Wei, 1990] which amounts to only 13 % for this case. The arguement for NMI as a contributing source for the emittance growth is strengthened by the sudden growth of high-harmonic beam current components as seen in the sample of harmonics in the range 300 – 319 shown in the second plot following.

Table II: **Fermilab Booster Parameters at Transition**

Parameter	Symbol	
Circumference	C	474.2 m
transition energy/$m_\circ c^2$	γ_T	5.110 GeV
rf peak voltage	V_{rf}	690 kV
rf harmonic	h	84
beam circulation frequency	$f_\circ$	621.5 kHz
ramp rate	$\dot{\gamma}$	419.2 s^{-1}
synchronous phase	ϕ_{s}	11.61 deg
nonadiabatic time	T_{na}	0.2572 ms
beampipe radius	b	8.0 cm
beam radius	a	1.38 cm
geometric factor	$g_\circ$	4.515
harmonic of $f_\circ$ for $g = \frac{1}{2}g_\circ$	$n_{1/2}$	23708
number of protons per bunch	N	$6.0 \cdot 10^{10}$
average bunch current	$\bar{I}_{\mathsf{bunch}}$	0.504 A
predicted nonlinear growth	$\frac{\Delta\epsilon}{\epsilon}$	0.128

Booster Emittance Throughout Acceleration Cycle

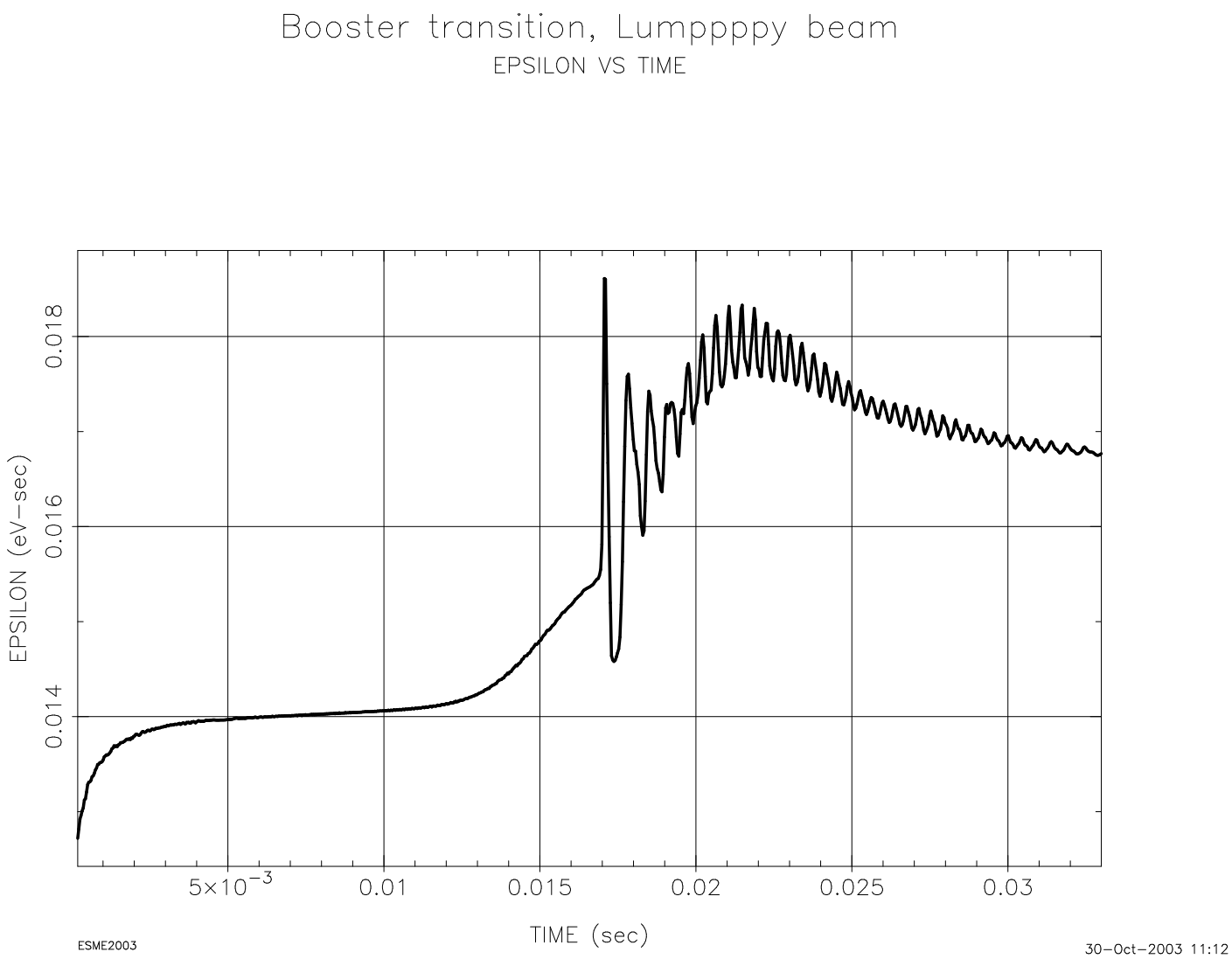

RMS emittance [eVs] *vs*. time [s] for a high intensity ($5 \cdot 10^{12}$ protons total) cycle in the Fermilab Booster injector synchrotron with current typical parameters. The irregularity in the later part of the plot reflects particle loss coming from nonlinear single particle effect in addition to the sudden emittance growth caused by NMI.

RMS Amplitude harmonics 300-319 Throughout Acceleration Cycle

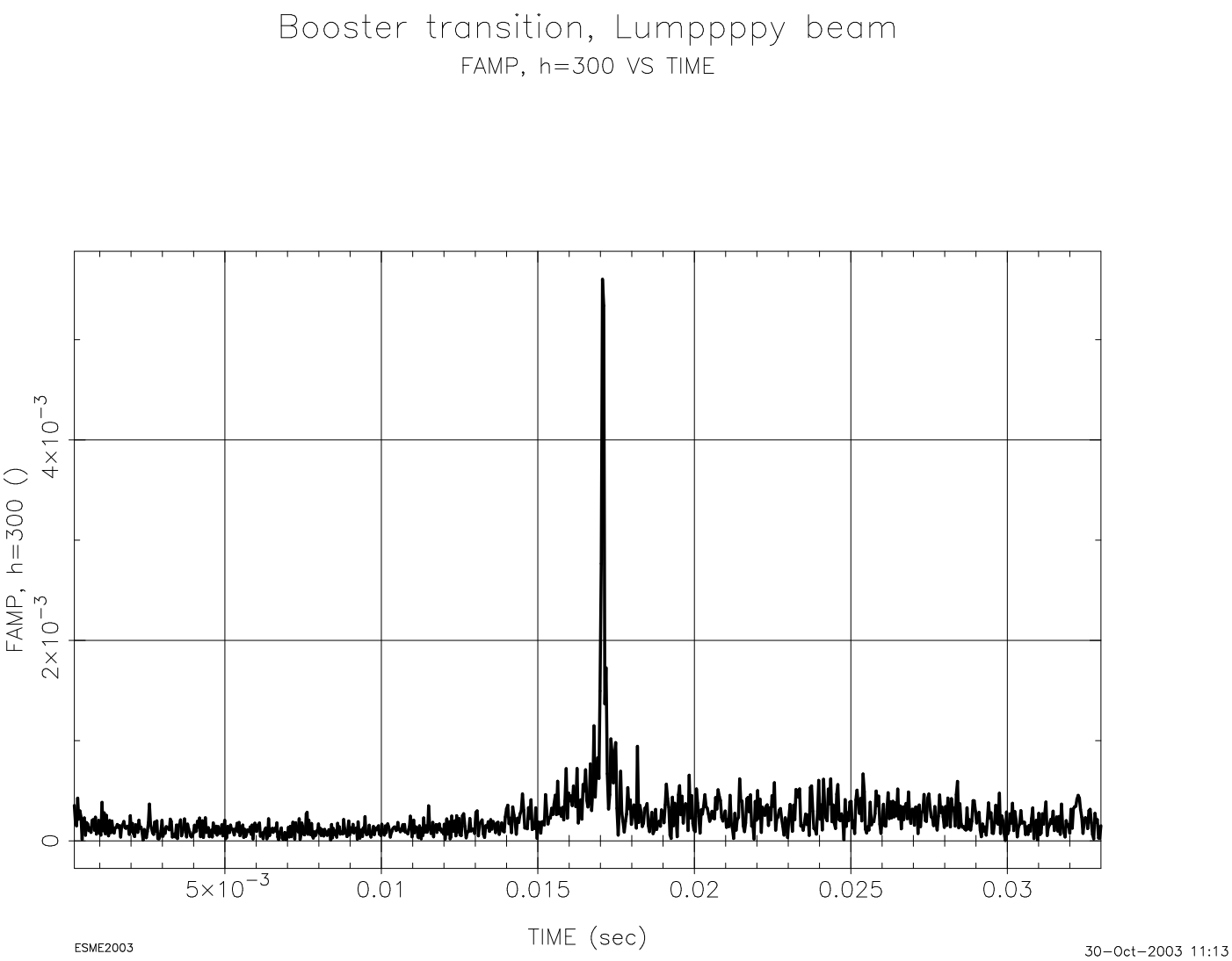

The rms of normalized beam charge amplitudes for harmonics 300 to 319 *vs*. time [s] during Booster acceleration cycle. Note the sudden appearence of these high harmonics just at transition time.

γ_T Jump - A Classic Fix

For the several problems in crossing transition several ameliorants have been developed, but the first broadly successful approach has been to cross the transition energy very rapidly by pulsing fast quadrupoles to move E_T downward through the beam energy far faster than the beam is accelerated in the basic machine cycle. Such an E_T change can not be arbitrarily large or fast, however, so the degree of improvement depends on details of what kind of system is practical for a particular accelerator lattice. Using parameters of the currently installed Booster γ_T system [W. Merz *et al*., 1987], the combined effects of single-particle nonlinearity and NMI are controlled rather well. The jump is not used routinely because of additional requirements on Booster operation, but increase in beam brightness will almost certainly require that operational problems with the system be resolved. The following plot of rms emittance *vs*. time is made under the same general conditions as the preceding plot except that the jump system is used with its nominal specifications.

Booster Emittance with γ_T Jump

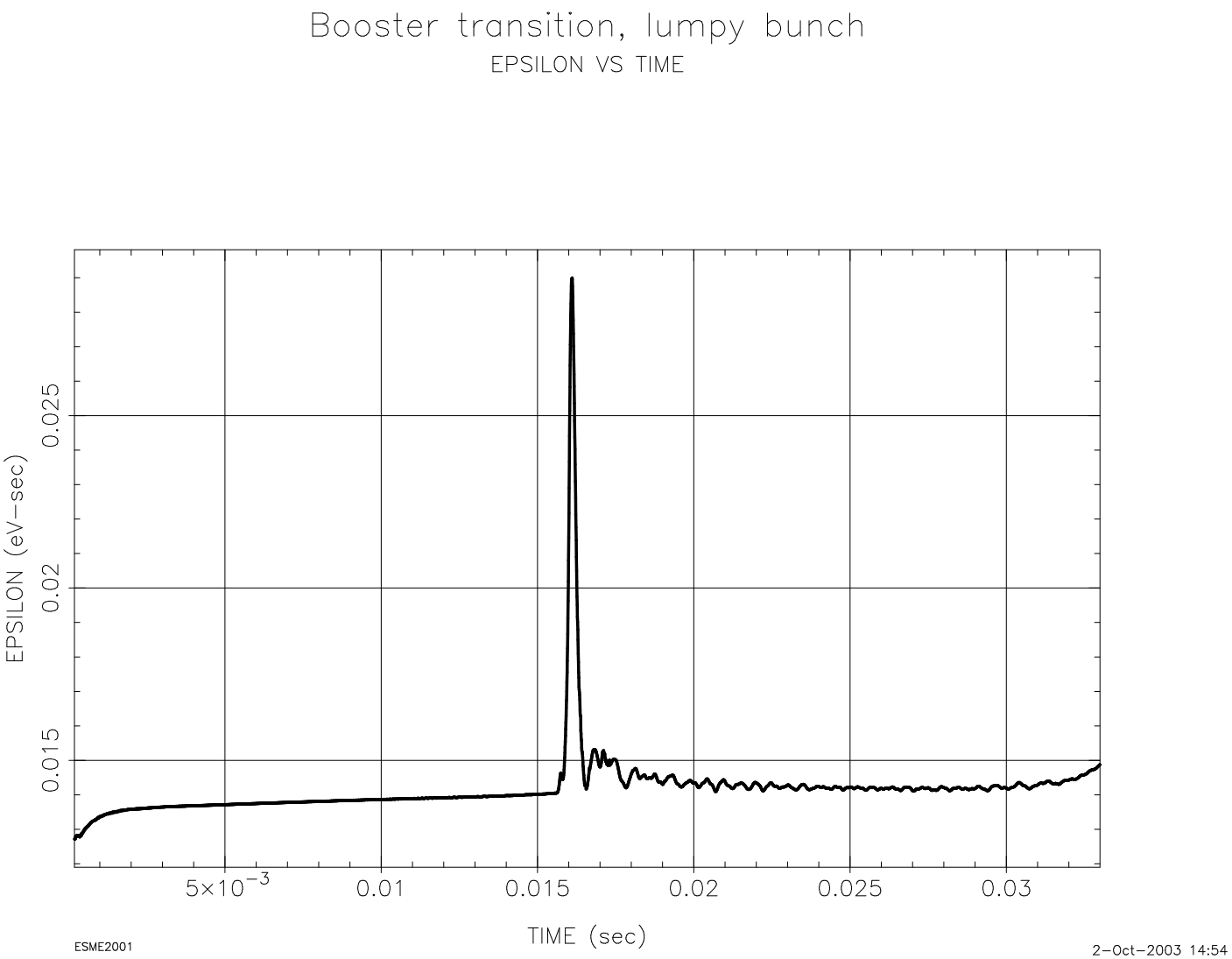

RMS emittance [eVs] *vs*. time [s] for a high intensity ($5 \cdot 10^{12}$ protons total) cycle in the Fermilab Booster injector synchrotron with the installed γ_T system operative. The emittance spike near the time of the jump, 15.5 ms, reflects the increase from a few particles soon lost. Note, however, that even the spike is relatively small and the final emittance is hardly changed from the initial.

Acknowledgements

My thanks to Jean-François Ostiguy for guidance and encouragement in the parallelization of ESME and general remarks echoed in this talk.

References

1. W. Hardt, “GAMMA-TRANSITION-JUMP SCHEME OF THE CPS”, in $9^{\underline{th}}$*Int’l Conf. High Energy Accel*., SLAC (1974) pp 434–438

2. J. A. MacLachlan, “ESME at 18: Realistic numerical modeling of synchrotron motion”, in $17^{\underline{th}}$ *Int’l Conf. High Energy Accel.*, JINR, Dubna, September 1998

3. J. Wei, “Longitudinal Dynamics of the Non-Adiabatic Regime on Alternating Gradient Synchrotrons”, PhD dissertation for State University of New York at Stony Brook (1990)

4. W. Merz, C. Ankenbrandt, and K. Koepke, “TRANSITION JUMP SYSTEM FOR THE FERMILAB BOOSTER”, USPAC 1987, IEEE cat. no. 87CH2387-9, pp 1343–1345